Scintillator Requirements for Medical Imaging*

William W. Moses

Lawrence Berkeley National Laboratory, University of California, Berkeley, CA 94720 USA

Scintillating materials are used in a variety of medical imaging devices. This paper presents a description of four medical imaging modalities that make extensive use of scintillators: planar x-ray imaging, x-ray computed tomography (x-ray CT), SPECT (single photon emission computed tomography) and PET (positron emission tomography). The discussion concentrates on a description of the underlying physical principles by which the four modalities operate. The scintillator requirements for these systems are enumerated and the compromises that are made in order to maximize imaging performance utilizing existing scintillating materials are discussed, as is the potential for improving imaging performance by improving scintillator properties.

Keywords: Medical Imaging, Planar X-Ray, X-Ray CT, SPECT, PET

1. Introduction

The first medical image is arguably the x-ray image that Röntgen took of his wife's hand in 1895. While Roentgen used photographic film to convert the x-rays into a form observable by the human eye, within one year powdered phosphor materials such as $CaWO_4$ replaced photographic film as the x-ray conversion material [1, 2], and have been an integral part of medical imaging devices ever since. In fact, virtually all medical imaging modalities that require the detection of energetic photons (x- and γ- rays) use scintillators for their detection. These modalities include planar x-ray imaging, x-ray computed tomography (x-ray CT), SPECT (single photon emission computed tomography) and PET (positron emission tomography).

The volume of scintillator required each year for medical imaging devices is considerable. Table 1 estimates the number of medical imaging units sold annually and the typical amount of scintillator in each kind of unit. All in all, about 175 metric tons of scintillator are required annually. The various medical imaging techniques that use scintillators all have different requirements. In principle, the ideal scintillator (one with extremely high density, high effective atomic number, high luminous efficiency, short decay time, no afterglow, good spectral match to photodetectors, and low cost) could be used for each application. However, the ideal scintillator does not exist and so each modality must compromise, choosing from available materials the most suitable combination of properties. The purpose of this paper is to describe the physical basis of the four medical imaging modalities listed in the paragraph above, the requirements for the scintillator in these modalities, the scintillators presently used by each of them, and the improvements in scintillator properties that would most benefit each application.

Modality	Annual Production	Scintillator Content	Annual Scint. Volume
Planar X-Ray	1,000,000 screens	50 cc / screen	50,000 liters
X-Ray CT	2,000 scanners	75 cc / scanner	150 liters
SPECT	2,000 scanners	3,000 cc / scanner	6,000 liters
PET	50 scanners	10,000 cc / scanner	500 liters

Table 1. Annual world-wide volume of scintillator required by medical imaging instruments.

* This work was supported in part by the U.S. Department of Energy under Contract No. DE-AC03-76SF00098, and in part by Public Health Service Grants No. R01-CA48002, R01-CA67911, and P01-HL25840 from the National Institutes of Health.

2. General Considerations

In all the systems considered in this paper, it is necessary to image photons whose energy is between 15 keV and 511 keV. The detection system must be very efficient, as safety concerns cause regulatory agencies to limit the total radiation dose that can be administered to a patient. Thus, reduced statistical noise cannot be obtained by increasing the source strength (*i.e.* the integrated x-ray flux or the injected activity), and so must be obtained by maximizing detection efficiency. At the 15–511 keV photon energies used for medical imaging, the attenuation length in tissue is 2–10 cm. This is similar to the distance that gamma rays need to travel to exit the body, so a significant fraction of the internally emitted gamma rays interact within the patient. Due to the low effective atomic number of tissue, most of these interactions result in Compton scatter, and most of the scattered photons continue to undergo Compton scattering until they leave the body. While the net radiation flux impinging upon the detector usually contains 10%–50% unscattered gammas (which can be used to form an accurate image), the majority are Compton photons that form a background. Thus, the detection system must be capable of reducing this Compton background, usually by physical collimation or by measuring the energy of each detected photon with 8%–20% full-width at half-maximum (fwhm) resolution.

X-ray CT, SPECT, and PET make use of the mathematical technique of computed tomography [3-5]. Briefly stated, computed tomography is a process whereby a 2-dimensional image of an object is formed using multiple 1-dimensional projection images of that object. This is demonstrated in Figure 1. The 2-dimensional object in question is a large circle of uniform density in which a medium circle of lower density and a small circle of higher density are embedded. The one dimensional projection of the object in the vertical direction is shown below the object. This projection is what would result if a planar x-ray of the object were taken, and represents the line integral of the 2-dimensional object's density along parallel, vertical lines that cross the object. The hemisphere corresponding to the large circle is clearly seen, modified by a dip due to the low density region and a spike due to the high density region. To the right of the object is its one dimensional projection in the horizontal direction. Again the hemisphere with the associated dip and spike are seen, but the positions of the dip and spike have changed because of the change in viewing angle. While the details are beyond the scope of this paper, taking one dimensional projections at all angles around an object (not just the two shown in Figure 1) provides enough information to reproduce a 2-dimensional image of the object.

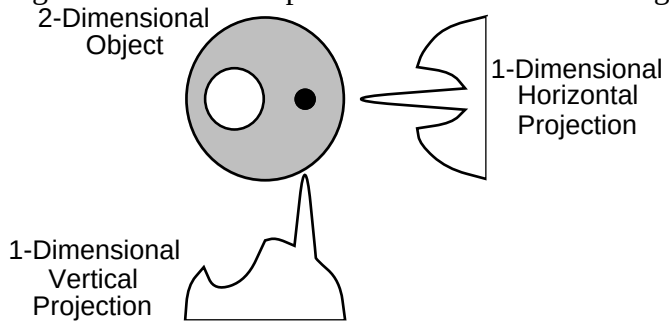

FIGURE 1. Computed Tomography. The 1-dimensional horizontal and vertical projections (the line integral of the density along parallel horizontal and vertical lines) are shown adjacent to the 2-dimensional object that they were taken of. Computed tomography is the process of reconstructing the 2-dimensional object given its 1-dimensional projections from all angles.

3. Planar X-Ray Imaging

With planar x-ray imaging, x-rays are generated by accelerating an electron beam toward a metal cathode, where the impact creates bremsstrahlung photons. These x-ray photons have a broad range of energies, with a mean energy of approximately half that of the incident electron energy (which is determined by the accelerating voltage). Depending on the body part to be imaged, this voltage is from 25 kV to 300 kV, resulting in individual x-ray energies ranging from approximately 15 keV to 200 keV. The x-rays undergo differential absorption as they penetrate the body, and the emerging x-ray flux is measured to form an image. As the incident x-ray flux is not monochromatic, there is little additional information (such as the identification of

Compton scattered photons) that can be obtained by measuring the energy. This, coupled with the high x-ray fluxes (10^{10} / sec / mm^2), dictate that individual quanta are not measured, and detectors that integrate the flux for the duration of the x-ray exposure are used.

Typical x-ray detector systems are shown in Figure 2 [6]. X-rays that penetrate the patient (and subsequent collimator) pass through a sheet of photographic film and strike a phosphor (powdered scintillator) screen. The subsequent scintillation photons expose the photographic film, which is mechanically separate from (although adjacent to) the phosphor screen. The film is then removed and chemically developed to form an image. Where possible, the x-rays are incident from the film side of the phosphor screen because of their exponential attenuation in the screen — with this geometry the maximum number of x-rays stop at the surface closest to the film. The scintillation photons undergo multiple scatters due to the powdered scintillator grains. This limits the lateral spread of the scintillation light (as compared to what would be obtained with a large, optically clear scintillator plate) and so enhances the spatial resolution. However, the lateral spread increases with increasing phosphor plate thickness, so applications that require high spatial resolution (such as mammography) use thin phosphor screens. In addition, spatial resolution can be degraded by scintillation photons that pass through the emulsion and are reflected at the back surface of the film substrate and then detected by the emulsion. This effect can be minimized either by an absorptive coating on the back surface of the film substrate or a dye in the film substrate that absorbs the scintillation light.

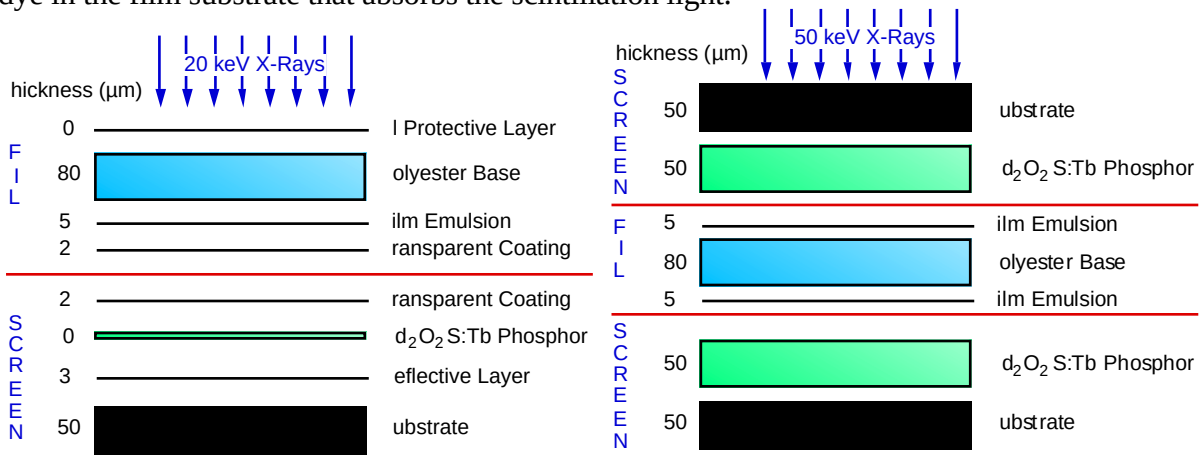

FIGURE 2. X-ray film / screen combination. The design at the left is for mammography, which requires extremely high spatial resolution. Specific resolution-enhancing features include thin scintillator screen and emulsion only on the side of the film substrate adjacent to the phosphor screen. The design at the right is for chest x-rays, which requires extremely high detection efficiency. Specific efficiency-enhancing features include dual, thick phosphor screens and emulsion on both sides of the film substrate.

The left side of Figure 2 shows a film / screen system that is optimized for spatial resolution, such as is used for mammographic applications which require high (~75 µm) spatial resolution when imaging low energy (~20 keV) x-rays. Such systems typically utilize a single, 12~µm thick phosphor screen and photographic film with emulsion on a single side. The opposite trade-off is found in chest x-ray systems, such as shown on the right side of Figure 2, which must be extremely efficient for imaging higher energy (~150 keV) x-rays. These systems have thicker (250 µm) phosphor screens placed on either side of the photographic film, which has emulsion on both sides.

The requirements for x-ray phosphors are, in order of decreasing importance, (1) high luminous efficiency (>60,000 photons/MeV), (2) high density (>7 g/cm^2), (3) emission wavelength well matched to the peak response wavelength of the photographic film (550 nm), (4) good particle shape (roughly spherical, 3–10 µm in diameter), and (5) good manufacturing properties (such as the ability to be made into a slurry without clumping). Table 2 lists the commonly used x-ray phosphors, as well as some of their relevant properties [7]. The Gd_2O_2S:Tb material is almost universally used due to its excellent combination of properties.

Material	Luminosity (photons/MeV)	Density (g/cm^3)	Wavelength (nm)	Shape
Gd_2O_2S:Tb	70,000	7.3	545	Good
LaOBr:Tb	67,000	6.3	425	Plate
Y_2O_2S:Tb	60,000	4.9	545	Good

Table 2. Materials used for planar x-ray imaging and their properties.

Opportunities for improving the scintillators used for planar x-ray imaging are somewhat limited as they are already near the theoretical limits. However, there is a need for higher x-ray "speed" in order to reduce the radiation dose to patients — many imaging procedures produce skin burns on the patient from the x-rays. In this context, "speed" does not refer to decay time, but is analogous to its definition for photographic film. That is, it refers to (the inverse of) the length of time necessary to achieve a proper exposure, given a fixed incident photon flux (and assuming a given image quality). A 10% increase in the speed is considered a very significant improvement. Such an increase could come from increased luminescent efficiency, decreased attenuation length, or development of microscopic scintillator structures (such as columnar CsI:Tl) that decrease the lateral light spread for a given screen thickness. It is also possible that development of phosphors whose emission wavelength is optimized for detection by silicon detectors (such as CCD's or amorphous silicon flat panel devices) would be useful. Electronic (as opposed to film based) readout of phosphors is an active area of research, and phosphors with 600–1000 nm emission wavelengths (and their higher number of emitted photons for a given energy conversion efficiency) would help these efforts.

4. X-Ray CT

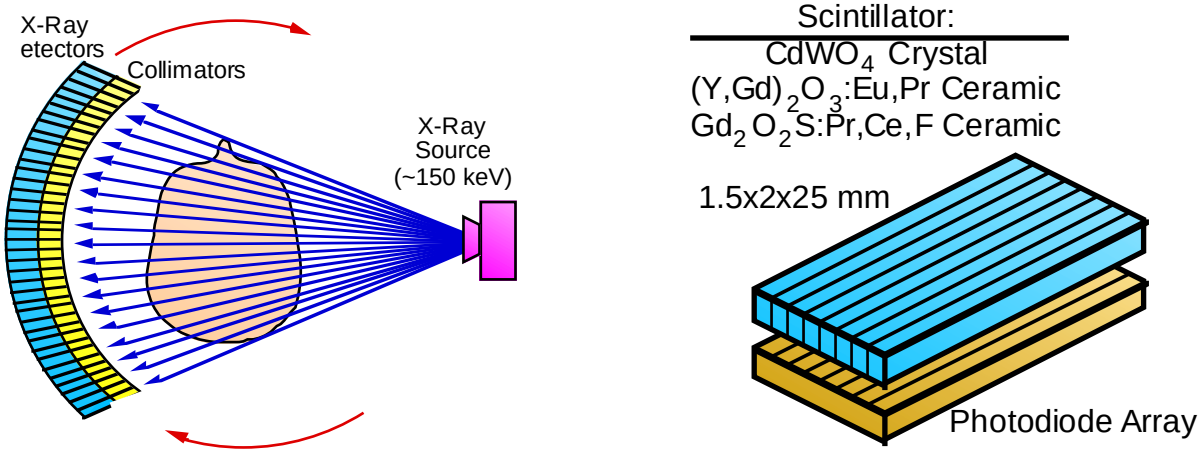

FIGURE 3. X-ray computed tomography system. On the left, an x-ray source illuminates the patient, while septa in front of the detectors reduce Compton scattered events. The source and detection system orbit around the patient. On the right is a typical detection system, consisting of scintillator crystals read out by photodiodes.

An x-ray CT system, as shown in Figure 3, consists of an x-ray source and an arc of individual x-ray detectors that monitor the transmitted x-ray flux [6]. As with planar x-ray imaging, the combination of the high x-ray photon flux and lack of a monochromatic source dictate that the energy of individual quanta are not measured, and so mechanical collimation is used to reduce Compton scatter. The entire assembly rotates around the patient (with a period of approximately 2 s), continuously moving but acquiring data in ~1 ms intervals. Typical x-ray detector elements, also shown in Figure 3, consist of crystalline or ceramic scintillator materials individually coupled to a photodiode. The output of the photodiodes (*i.e.* the current) is digitized with typically 20 bit dynamic range. Computed tomography, as described earlier, is used to convert this data into cross-sectional images of the patient, which are then stacked to form a 3-dimensional volumetric image.

The technique of computed tomography essentially makes use of the small systematic differences in nearly adjacent views to create an image. With x-ray imaging, these differences can be quite small, requiring that the transmitted flux be measured with 1–10 ppm (parts per million) accuracy. Such high accuracy implies that systematic errors must be rigorously controlled, both by minimizing the sources of error and by software corrections of the remaining errors. Such errors include beam hardening (the fact that the absorption coefficient μ is energy dependent and the x-ray beam is not monochromatic implies that the high energy portion of the x-ray spectrum is attenuated less than the low energy portion), x-ray tube drift (caused by x-ray tube acceleration voltage fluctuations and motion from cathode deformation caused by electron beam heating), and partial volume effect (the fact that each voxel in the patient does not contain material with a single, uniform μ value). Systematic effects from the scintillator that must be minimized include afterglow (decay components that extend beyond the 1 ms integration time), temperature dependence, and radiation damage (at the 10 rad level) [8]. Ceramic materials often show more uniformity than crystalline materials, as by nature they "average" the properties of many (very small) scintillator crystals.

The requirements for x-ray CT scintillators are, in order of decreasing importance, (1) low afterglow (<1% @ 3 ms), (2) high stability (chemical, temperature, and radiation damage), (3) high density (>6 g/cm^2), (4) emission wavelength well matched to photodiode readout (500–1000 nm), and (5) high luminous efficiency (>15,000 photons/MeV). Table 3 lists the commonly used scintillators for x-ray CT, as well as some of their relevant properties [9]. All three of the materials listed are presently used in commercial CT scanners. It is interesting to note that several of the materials have more than one dopant. In general, the first dopant is a luminescent ion, while the subsequent dopants are used to reduce the afterglow.

Material	Luminosity (photons/MeV)	Density (g/cm^3)	Decay (μs)	Afterglow (@ 3 ms)	Form
$CdWO_4$	14,000	7.9	5, 20	<0.1%	Crystal
$(Y,Gd)_2O_3$:Eu,Pr	19,000	5.9	1000	3%	Ceramic
Gd_2O_2S:Pr,Ce,F	21,000	7.3	3	<0.1%	Ceramic

Table 3. Materials used for x-ray CT imaging and their properties.

There are significant opportunities for improving the scintillators used for x-ray CT imaging, as none of the properties (with the possible exception of the density) are already near fundamental theoretical limits. The most desired improvements would be in the density and the stability, particularly with regards to radiation damage and temperature dependence of the luminous efficiency. Increase in the luminous efficiency is not deemed important, as the statistical noise is dominated by counting statistics of the incident flux, not the x-ray / photodetector response. Some of the individual materials could use improvement in specific areas. For example, the $(Y,Gd)_2O_3$:Eu,Pr material would significantly benefit from a shorter decay time, while the Gd_2O_2S:Pr,Ce,F material would benefit from improved optical transparency. Finally, the fact that there are three commercially accepted materials (rather than one dominant material) suggests that the best properties of each material might be combined to create an improved material.

5. SPECT

Nuclear medical imaging is a generic term that covers many imaging techniques, with the common theme being that ionizing radiation originating from within the body is detected and imaged in order to determine something about the physiology or anatomy of the subject [5, 6, 10-12]. With SPECT, a biologically active compound (*i.e.* a drug) is introduced into the body (in trace quantities) either by injection or inhalation. This compound then accumulates in the patient and the pattern of its subsequent radioactive emissions is used to estimate the distribution of the radioisotope and hence of the tracer compound. The radioisotopes used for SPECT are gamma ray emitters with monochromatic emissions between 60 keV and 511 keV, with the 140 keV emissions from ^{99m}Tc being the most common.

A typical SPECT camera is shown schematically in Figure 4. The emitted gamma rays are detected by two-dimensional position sensitive detectors. The direction of the gamma rays is determined by a collimator placed between the detector array and the patient — photons that are not traveling in the desired direction are absorbed by the collimator. The collimator and detector combination (and their associated electronics and mechanical support) form what is known as a gamma camera "head". While multiple heads increase the detection efficiency of a SPECT camera (and the cost), there is little efficiency gain above three heads, so most SPECT cameras have between one and three heads. Each head measures a planar projection of the activity in the patient, and by simultaneously rotating the heads, the requisite set of projections to perform computed tomography is obtained.

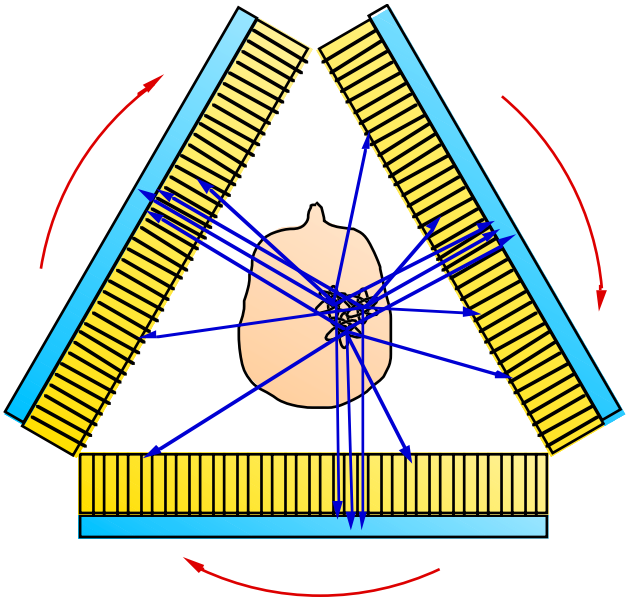

FIGURE 4. SPECT Camera Schematic. A collimator blocks gamma rays that are not traveling normal to its surface, and those gammas that pass through the collimator are detected with a planar position sensitive detector. The assembly rotates around the patient to provide the many projections necessary for computed tomography.

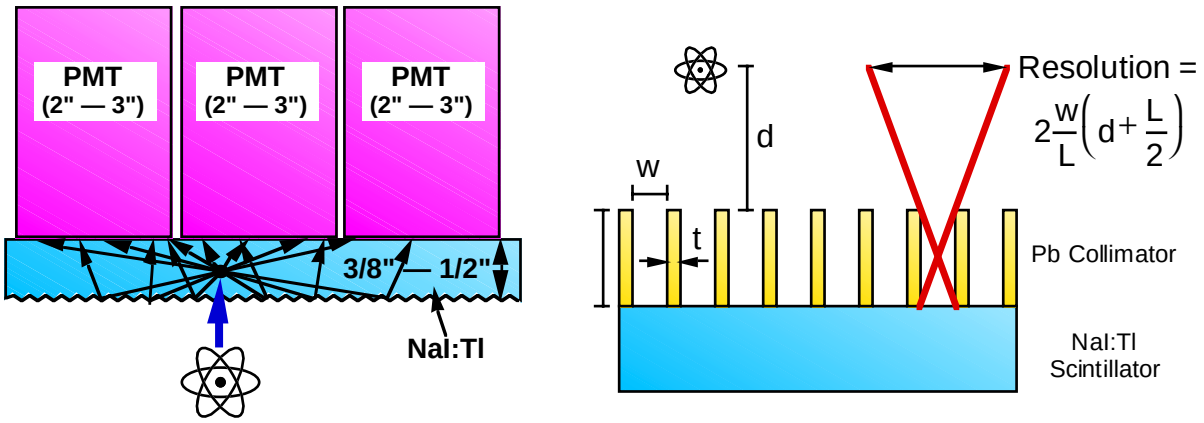

FIGURE 5. Anger Camera. Scintillation light from gamma ray interactions is detected by multiple photomultiplier tubes. The interaction position is determined by the ratio of the analog signals, and the energy by the analog sum of the signals.

The most commonly used gamma detector for SPECT is the Anger camera, which is named for its inventor [13]. A schematic of an Anger camera is shown in Figure 5. A plate of NaI:Tl scintillator crystal is optically coupled to many photomultiplier tubes. When a gamma ray interacts in the crystal, the resulting scintillation photons are emitted isotropically and are detected by several of the photomultiplier tubes. The position of the gamma ray interaction is then determined by the analog ratio of the photomultiplier tube output signals, and the gamma ray energy is determined by the sum of these signals. The accuracy of the position measurement is improved with increasing scintillator luminous efficiency.

The thickness of the NaI:Tl crystal determines the efficiency of the camera. As its attenuation length for 140 keV gamma rays is 4 mm, the 9–12 mm thick plates commonly employed in SPECT systems provide nearly complete absorption. The scintillator surface not coupled to the photomultiplier tubes strongly affects the light distribution observed by the photomultiplier tubes and is often prepared with a proprietary surface treatment to optimize both position and energy resolution. Care is needed near the edges of the scintillator crystal, as reflections from the side of the crystal cause the dependence of the measured light distribution on the interaction position to be much weaker near the sides than near the middle. A typical Anger camera has 9% fwhm energy resolution and 3.5 mm fwhm position resolution for 140 keV gammas.

While the Anger camera is an important component of a SPECT imager, the performance of a SPECT camera is almost entirely determined by the collimator [14]. The collimator is usually made from cast lead with hexagonal cross section holes arranged in a honeycomb fashion. Each hole can be thought of as having a diameter w and a length L, separated from its neighbors by a lead septum of thickness t (typically 0.2 mm). The spatial resolution is determined by the collimator geometry and is given by

$$\text{Resolution} = 2\frac{w}{L}\left(d + \frac{L}{2}\right), \qquad (1)$$

where d is the distance from the collimator surface to the object being imaged. From Equation 1 we can see that the resolution scales linearly with the aspect ratio w/L of the collimator, and as L is typically 1–3 cm and d is typically tens of centimeters, increases roughly linearly with the distance d from the collimator. While arbitrarily high spatial resolution can be achieved with a collimator by reducing w/L, more modest spatial resolution is usually obtained because this aspect ratio greatly affects the efficiency. The fraction of gammas that are transmitted through the collimator is

$$\text{Efficiency} = \left(\frac{w}{2L}\right)^2, \qquad (2)$$

so while the resolution improves linearly with w/L, the efficiency decreases quadratically. For a typical "all-purpose" collimator, the spatial resolution is 6.2 mm fwhm at a distance of 5 cm and the efficiency is 0.023%. From this we see that the spatial resolution of a SPECT image is not determined by the resolution of the Anger camera (which is known as the intrinsic resolution), but by the collimator.

Material	Luminosity (photons/MeV)	Density (g/cm^3)	Decay Time (ns)	Wavelength (nm)
NaI:Tl	38,000	3.7	230	415
CsI:Tl	60,000	4.5	1000	545

Table 4. Materials used for SPECT imaging and their properties.

The scintillator requirements for SPECT are, in order of decreasing importance, (1) high luminous efficiency (for good energy resolution and intrinsic spatial resolution), (2) high density (>3.5 g/cm^3), (3) low cost (<\$15/cm^2, where the area referred to is the surface area around the patient that must be surrounded with 3 attenuation lengths of scintillator), (4) an emission wavelength well matched to photomultiplier tube readout (300–500 nm), and (5) short decay time (<1 μs). Table 4 lists the commonly used scintillators for SPECT, as well as some of their relevant properties. Virtually the only material in use is NaI:Tl — CsI:Tl is only used in experimental devices employing photodiode (rather than photomultiplier tube) readout.

There are some opportunities for improving the scintillators used for SPECT imaging. The most desirable improvements would be increased luminous efficiency. This would improve the energy resolution from its present 9% fwhm for 140 keV gamma rays, and also allow the same intrinsic resolution to be achieved with fewer (but larger) photomultiplier tubes.

6. PET

PET (Positron Emission Tomography) [15] is similar to SPECT, in that a radioactively labeled drug is imaged, but PET employs radioisotopes that are positron emitters. The emitted positron rapidly thermalizes in the patient's tissue, attracts an electron, and annihilates to form back-to-back 511 keV photons. A typical PET camera, shown schematically in Figure 5, consists of a planar ring of small photon detectors, with each photon detector placed in time coincidence with *each* of the individual photon detectors on the other side of the ring. When a pair of photon detectors simultaneously detect 511 keV photons, a positron annihilated somewhere on the line connecting the two detectors. The method of using time coincidence between two detectors (rather than a collimator and one detector) to restrict events to a line is known as electronic collimation, and is much more efficient than the mechanical collimation used in SPECT.

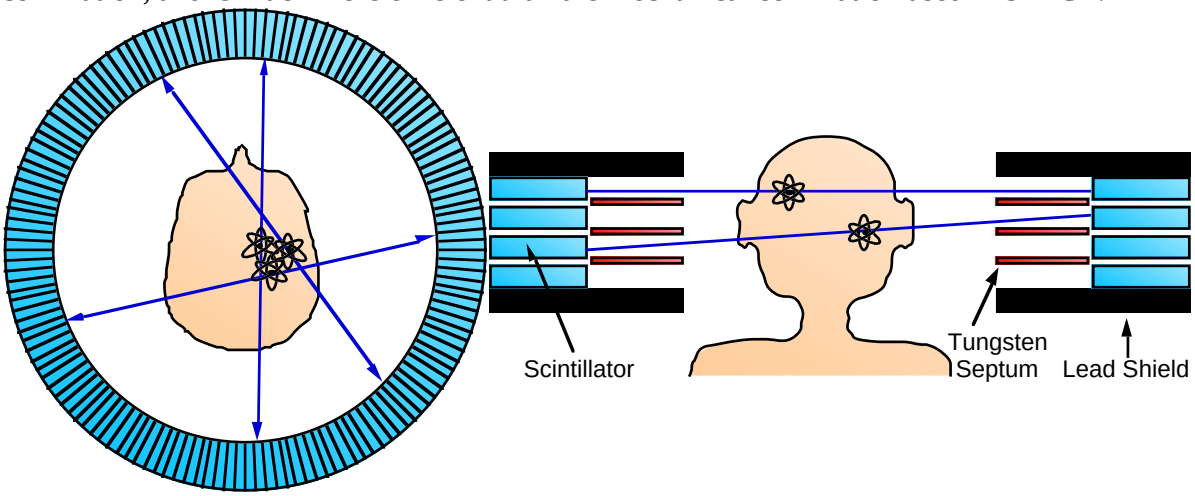

FIGURE 5. PET Camera Schematic. Positron annihilations yield back to back 511 keV photons, which are individually detected in a ring of photon detectors, shown on the left. Pairs are identified by time coincidence. Multiple rings are stacked up, as shown on the right, to create a 3-dimensional image.

The set of all lines connecting detectors (known as chords) makes the requisite set of projections to perform computed tomography for a single plane. Multiple detector rings are stacked on top of each other to obtain images from multiple slices, and thus a three-dimensional image of the patient. Planes of tungsten septa placed between detector planes are often used to shield the detectors from Compton scattered photons emanating from other parts of the body, and images taken in this geometry are often known as "2-D PET" images. Coincidences between nearly adjacent "cross-plane" rings are usually added to the closest "direct plane" to increase detection efficiency. If the septa are removed, the efficiency is greatly increased (as coincidences from widely separated planes can be accepted), but the backgrounds also increase significantly. However, the signal to noise ratio improves in some situations, and this mode of operation is known as "3-D PET."

The most commonly used PET detector module is known as a block detector, and a schematic is shown in Figure 3 [16]. A block of BGO scintillator crystal is partially sawn through to make a group of quasi-independent crystals that are optically coupled to four photomultiplier tubes. When a gamma ray interacts in the crystal, the resulting scintillation photons are emitted isotropically but the saw cuts limit (but do not entirely prevent) their lateral dispersion as they travel toward the photomultiplier tubes. The position of the gamma ray interaction is then determined by the analog ratio of the photomultiplier tube output signals, and the gamma ray energy is determined and a timing pulse generated by the sum of these signals.

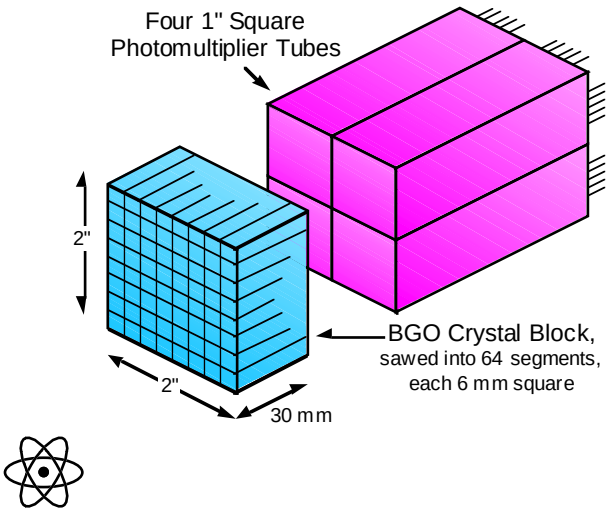

FIGURE 6. PET Detector Module. Scintillation light from gamma ray interactions is detected by multiple photomultiplier tubes. The interaction position is determined by the ratio of the analog signals, and the energy by the analog sum of the signals.

The thickness of the BGO crystal determines the efficiency of the camera. As its attenuation length for 511 keV gamma rays is 1.2 cm, the 30 mm thick BGO crystals commonly employed in PET systems provide nearly complete absorption. The coincidence timing efficiency is limited by the decay time of BGO — the photoelectron (p.e.) rate immediately after a 511 keV photon interaction is approximately 0.5 p.e./ns. A typical PET detector module has 20% fwhm energy resolution, 2 ns fwhm timing resolution and 5 mm fwhm position resolution for 511 keV gammas.

The scintillator requirements for PET are, in order of decreasing importance, (1) short attenuation length (<1.2 cm), (2) short decay time (<300 ns), (3) low cost (<\$100/cm^2, where the area again is that area surrounding the patient that must be covered with a 3 attenuation length thick scintillator), (4) high luminous efficiency (>8,000 photons/MeV), and emission wavelength well matched to photomultiplier tube readout (300–500 nm). Table 5 lists the commonly used scintillators for PET, as well as some of their relevant properties [17]. The most common material in use is $Bi_4Ge_3O_{12}$ — Lu_2SiO_5:Ce is just beginning to be incorporated into PET scanners.

Material	Luminosity (photons/MeV)	Atten. Length (cm)	Decay Time (ns)	Wavelength (nm)
$Bi_4Ge_3O_{12}$	8,000	1.1	300	480
Lu_2SiO_5:Ce	25,000	1.2	40	420

Table 5. Materials used for PET imaging and their properties.

In contrast to the previously mentioned modalities, there are significant opportunities for improving the scintillators used for PET imaging. Substantial improvements in luminous efficiency (and hence energy resolution) and decay time (as compared to BGO) should be quite possible, as these are well away from the theoretically possible limits. LSO goes a long way toward closing this gap, but improvements beyond those possible with LSO (such as the energy resolution) would also be valuable.

7. Conclusions

Scintillators have been used for over 100 years to non-invasively image the interior of the human body. Many techniques in use today involve imaging photons with energies of 15–511 keV, as these photons can be produced by x-ray sources or radioisotope decay, penetrate the body with reasonable probability, and be detected with high efficiency and good spatial

resolution. Detectors for these applications have seen many years of development and refinement, and generally possess high detection efficiency (to maximize image quality for a given patient radiation dose), good energy resolution (to minimize background from Compton scatter in the patient), low cost (as there is a competitive commercial market for these devices), and good (75 μm–5 mm) spatial resolution. While the scintillator materials used for each imaging application are highly optimized, there is potential and desire for improvement (without violating theoretical or practical limits) for virtually applications.

8. Acknowledgments

I would like to acknowledge Dr. Stephen Derenzo, Dr. Thomas Budinger, and Dr. Ronald Huesman for many interesting conversations, Dr. Ruvin Deych for sharing his knowledge of x-ray CT, and Dr. James Colsher and Dr. Harold Kidd for their insights into the commercial aspects. This work supported in part by the Director, Office of Science, Office of Biological and Environmental Research, Medical Science Division of the U.S. Department of Energy under Contract No. DE-AC03-76SF00098, and in part by the National Institutes of Health, National Cancer Institute under grants No. R01-CA48002 and R01-CA67911, and National Institutes of Health, National Heart, Lung, and Blood Institute under grant No. P01-HL25840.

References

1. T.A. Edison. Nature (1986) 470.
2. M. Levy. Fortschr. auf dem Geb. d. Röntgenstrahlen 1 (1897) 75.
3. A.M. Cormack. J. Appl. Phys. 34 (1963) 2722–2727.
4. D.E. Kuhl and R.Q. Edwards. Radiology 80 (1963) 653–662.
5. A. Macovski. *Medical Imaging Systems* 1-256 (Prentice Hall, Englewood Cliffs, NJ, 1983).
6. E. Krestel. *Imaging Systems for Medical Diagnosis* 1-636 (Siemens Aktiengesellschaft, Berlin, 1990).
7. N. Miura. in *Phosphor Handbook* (eds. S. Shionoya & W. M. Yen) 521–537 (CRC Press, Boca Raton, FL, 1999).
8. R. Deych, J. Dobbs, S. Marcovici, *et al.* in *SCINT95: International Conference on Inorganic Scintillators and Their Applications* (eds. P. Dorenbos & C. W. E. van Eijk) 36–39 (Delft University Press, Delft, The Netherlands, 1995).
9. B.C. Grabmaier. in *Heavy Scintillators for Scientific and Industrial Applications* (eds. F. De Notaristefani, P. LeCoq & M. Schneegans) 65–74 (Editions Frontieres, Gif-sur-Yvette, France, 1993).
10. M.P. Sandler, R.E. Coleman, F.J.T. Wackers, *et al. Diagnostic Nuclear Medicine* 1-1549 (Williams & Wilkins, Baltimore, MD, 1996).
11. W.R. Hendee and R. Ritenour. *Medical Imaging Physics* 1-781 (Mosby Year Book, St. Louis, MO, 1992).
12. S. Webb. *The Physics of Medical Imaging* 1-633 (Institute of Physics Publishing, Bristol, 1993).
13. H.O. Anger. Rev. Sci. Instr. 29 (1958) 27–33.
14. B.M.W. Tsui, D.L. Gunter, R.N. Beck, *et al.* in *Diagnostic Nuclear Medicine* (eds. M. P. Sandler) 67–79 (Williams & Wilkins, Baltimore, MD, 1996).
15. S.R. Cherry and M.E. Phelps. in *Diagnostic Nuclear Medicine* (eds. M. P. Sandler) 139–159 (Williams & Wilkins, Baltimore, MD, 1996).
16. S.R. Cherry, M.P. Tornai, C.S. Levin, *et al.* IEEE Trans. Nucl. Sci. NS-42 (1995) 1064–1068.
17. W.W. Moses and S.E. Derenzo. in *Inorganic Scintillators and Their Applications* (eds. P. Dorenbos & C. W. E. van Eijk) 9–16 (Delft University Press, Delft, The Netherlands, 1996).